Supporting Information

Fluorescent sensor for rutin hydrate based on cyanostilbene macrocycle

1. General

Chemical reagents were purchased from Aladdin Reagent Company. The reaction process was detected by thin-layer chromatography and the products were purified by column chromatography on silica gel (200-300 mesh). NMR (nuclear magnetic resonance) spectra were acquired on a Bruker-ARX 400 instrument using TMS (tetramethylsilane) as an internal standard. Mass spectra (MS) were performed on a Bruker mass spectrometer. UV-vis spectra were measured on a Shimadzu UV-vis spectrometer. Fluorescence detection was performed on a Hitachi F-4500 spectrometer. Elemental analyses were analysed on Vario EL IIIElemental Analyzer. The fluorescence absolute values (Φ_F) were estimated on an Edinburgh Instruments FLS920 Fluorescence Spectrometer with a 6-inch integrating sphere. Compound **2** was synthesised according to a previous report (Ying Gong; Shuting Fang; Yijie Zheng; Hongyu Guo; Fafu Yang. Tetra-Cyanostilbene Macrocycle: An Effective "Turn-on" Fluorescence Sensor for Oxalic Acid in Aqueous Media. J. Photochem. Photobiol. A Chem. 2022,435,114307).

2 The experimental procedure of detecting rutin hydrate in the test paper and fruits

Pieces of neutral filter paper were immersed in DMSO-H_2O (5:95) solution of **BCM** (0.1 mM) for 2 minutes. After dryness under room temperature, these papers were cut into hexagonal star pattern. Then these hexagonal papers were added with 5 drops of different guest solutions (0.1 mM). Subsequently, after dryness at air again, the fluorescence for these papers was observed under UV_{365nm} light to obtain the fluorescence photographs. On the other hand, these papers were added with 5 drops of the solution of rutin hydrate in different concentrations (0.0 mM, 0.02 mM, 0.04 mM, 0.06 mM, 0.08 mM and 0.1 mM) (0.1 mM). Subsequently, after dryness at air again, the fluorescence for these papers was observed under UV_{365nm} light to obtain the fluorescence photographs.

Also, three fruits (namely kiwi, apple and grape) were ground, then ultrasonically shaken, allowed to stand and filtered with DMSO-H_2O (5:95) solvent. 1 mL of these solution was mixed with 1 mL of **BCM** solution (DMSO-H_2O (5:95), 1.0×10^{-4} M). The obtained mixed solution was then diluted to 10 mL by DMSO-H_2O (5:95) observed by UV_{365nm} light. Further, these solutions were examined by fluorescence spectra to evaluate the fluorescence intensity (λ_{ex} = 340 nm, λ_{em} = 475 nm), which was

further compared by the standard working curve (the equation in the inserted scheme in Figure 3b: $y_0 = 4314.8-3616.4x_0$). The values of x_0 were the concentration of rutin hydrate in these fruits solutions.

3   The experimental procedure of standard addition recoveries

The certain amount (1.0×10^{-5} M, 2.0×10^{-5} M and 3.0×10^{-5} M) of rutin hydrate was added in the solution of three fruits (namely kiwi, apple and grape) prepared in the procedure 2. On the other hand, 1.0×10^{-4} M of **BCM** solution was prepared in DMSO-H_2O (5:95). Then, 1.0 mL of prepared fruits solution in corresponding concentration was mixed with 1.0 mL of prepared **BCM** solution, following that the mixture was diluted to 10 mL by DMSO-H_2O (5:95). As a result, the concentration of **BCM** was 1.0×10^{-5} M, and the added concentrations of rutin hydrate were 1.0×10^{-6} M, 2.0×10^{-6} M and 3.0×10^{-6} M in these solutions, respectively. The obtained solutions were then examined by fluorescence spectra to evaluate the fluorescence intensity (λ_{ex} = 340 nm, λ_{em} = 475 nm), which was further compared by the standard working curve (the equation in the inserted scheme in Figure 3b: $y_1 = 4314.8-3616.4x_1$). The values of x_1 subtracted x_0 obtained in procedure 2 to give the added concentrations, which were filled as found concentration in Table 1. All data were perfomed by three independent experiments and the RSD were then calculated.

4   The synthetic process and characteristic spectra.
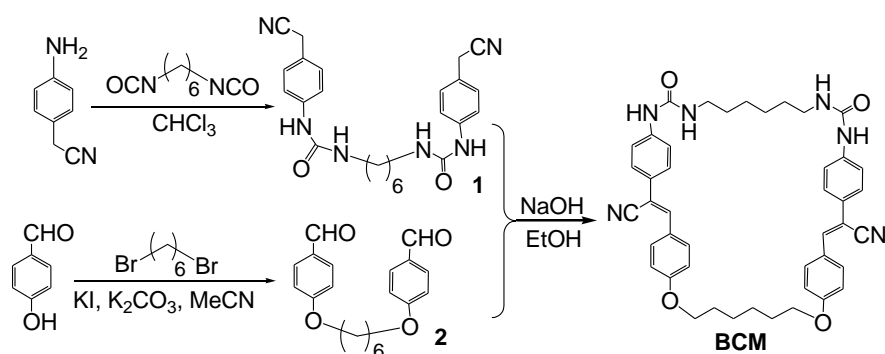
Scheme S1 The synthesis of target compound **BCM**

5   Synthesis of compound 1

A mixture of p-aminobenzeneacetonitrile (1.0 g, 7.6 mmol), hexamethylene diisocyanate was stirred and refluxed in 45 mL of dry trichloromethane for 15 h. Thin layer chromatography analysis was used to monitor the reaction. Then the reaction mixture was cooled and 50 mL of n-hexane was added in it. The solid precipitate was formed, filtered and dried. This crude product was further recrystallized in DMSO/MeOH (V/V = 1:10) to give white solid in 90% yield. ^{1}H NMR (400 MHz, DMSO) δ8.46 (s, 2H, ArNHCO), 7.39 (d, J = 8.0 Hz, 4H, ArH), 7.17 (d, J = 8.0 Hz, 4H, ArH), 6.15 (t, J = 4.0 Hz, 2H, CONH),

3.90 (s, 4H, CH_2CN), 3.06 (m, 4H, NCH_2), 1.42 (m, 4H, CH_2), 1.30 (bs, 4H, CH_2); MALDI-TOF-MS ($C_{24}H_{28}N_6O_2$) Calcd. For m/z= 432.23, found: 472.289 [M+Na$^+$].

6 Synthesis of BCM

The mixture of compound **1** (0.432 g, 1 mmol), compound **2** (0.326 g, 1 mmol) and NaOH (0.08 g, 2 mmol) was stirred and refluxed in 40 mL of anhydrous ethanol (99.5%) solution for 24 h. Thin layer chromatography was used to monitor the progress of the reaction. After reaction, the most of solvent was removed by reduced presssure. The residue was purified by rapid column chromatography (eluent: CH_2Cl_2 : MeOH = 5 : 1) to offer a light yellow solid in 75% yield. ^{1}H NMR (400 MHz, DMSO) δ8.68 (s, 2H, ArNHCO), 7.84 (d, J = 12.0 Hz, 4H, ArH), 7.76 (s, 2H, C=CHCN), 7.54 (d, J = 8.0 Hz, 4H, ArH), 7.47 (d, J = 8.0 Hz, 4H, ArH), 7.03 (d, J = 12.0 Hz, 4H, ArH), 6.23 (bs, 2H, CONHC), 4.02 (bs, J = 8.0 Hz, 4H, OCH_2), 3.05 (t, J = 8.0 Hz, 4H, NCH_2), 1.73 (bs, 4H, CH_2), 1.41 (s, 4H, CH_2), 1.28 (bs, 8H, CH_2). ^{13}C NMR (101 MHz, DMSO) δ 155.59, 140.55, 132.17, 131.26, 128.88, 126.45, 123.63, 120.02, 118.35, 115.33, 114.41, 107.45, 68.13, 63.03, 30.20, 26.61, 25.70, 22.48. MALDI-TOF-MS ($C_{44}H_{46}N_6O_4$) Calcd. For m/z= 722.358, found: 745.352 [M+Na$^+$]. Anal. calcd for $C_{44}H_{46}N_6O_4$: C 73.11, H 6.41, N 11.63; found C 73.14, H 6.38, N 11.59%.
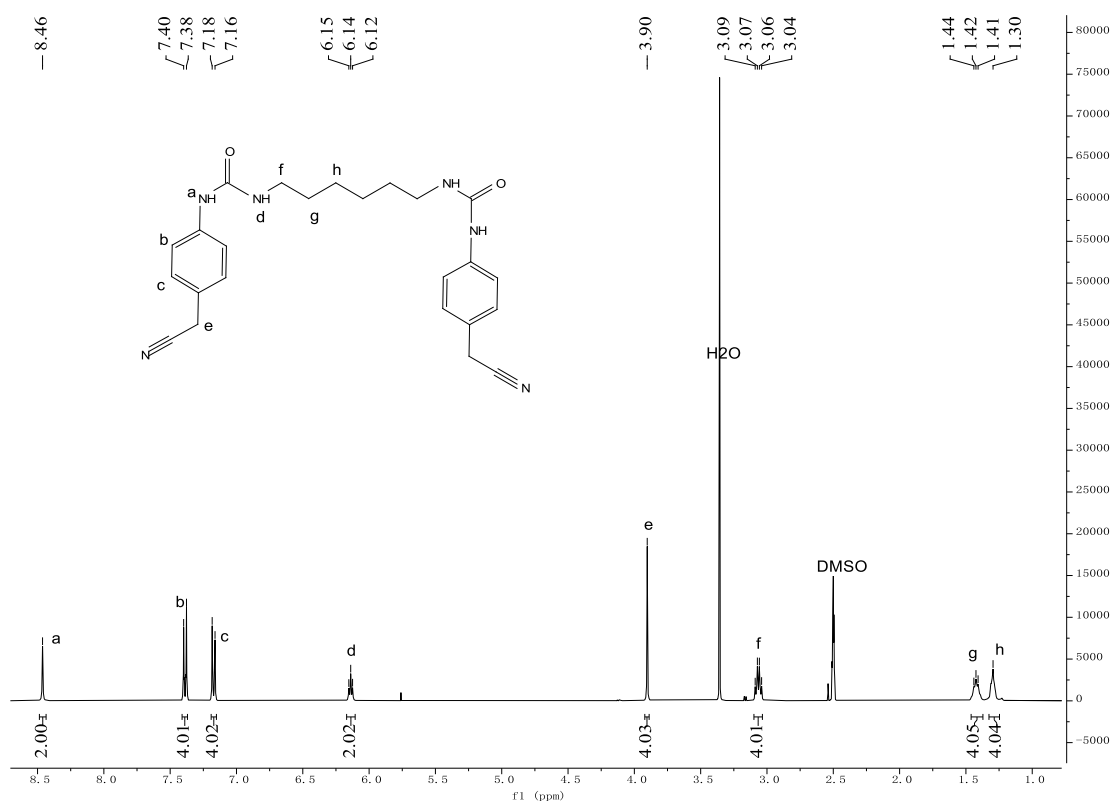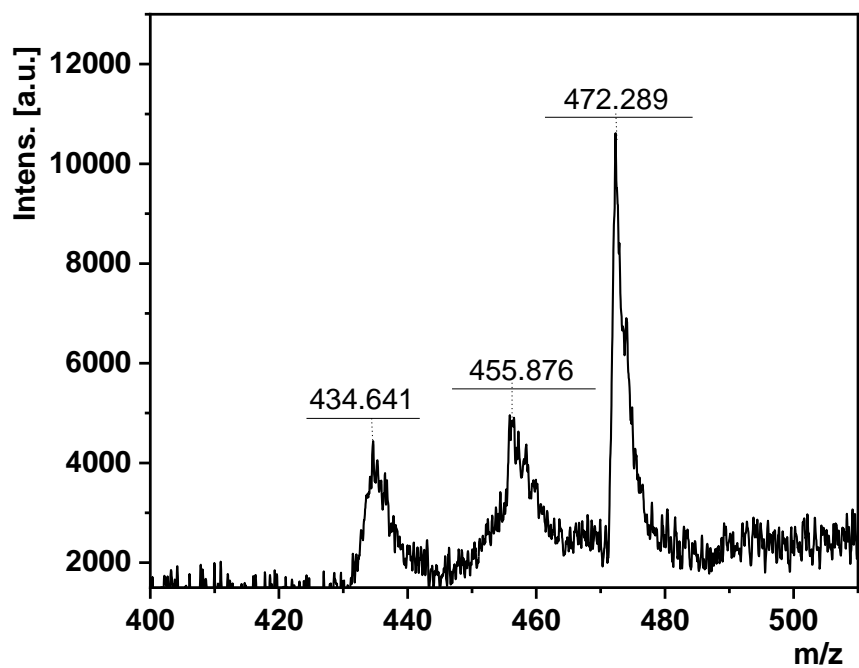

Figure S1 The ^{1}H NMR spectrum of compound **1**

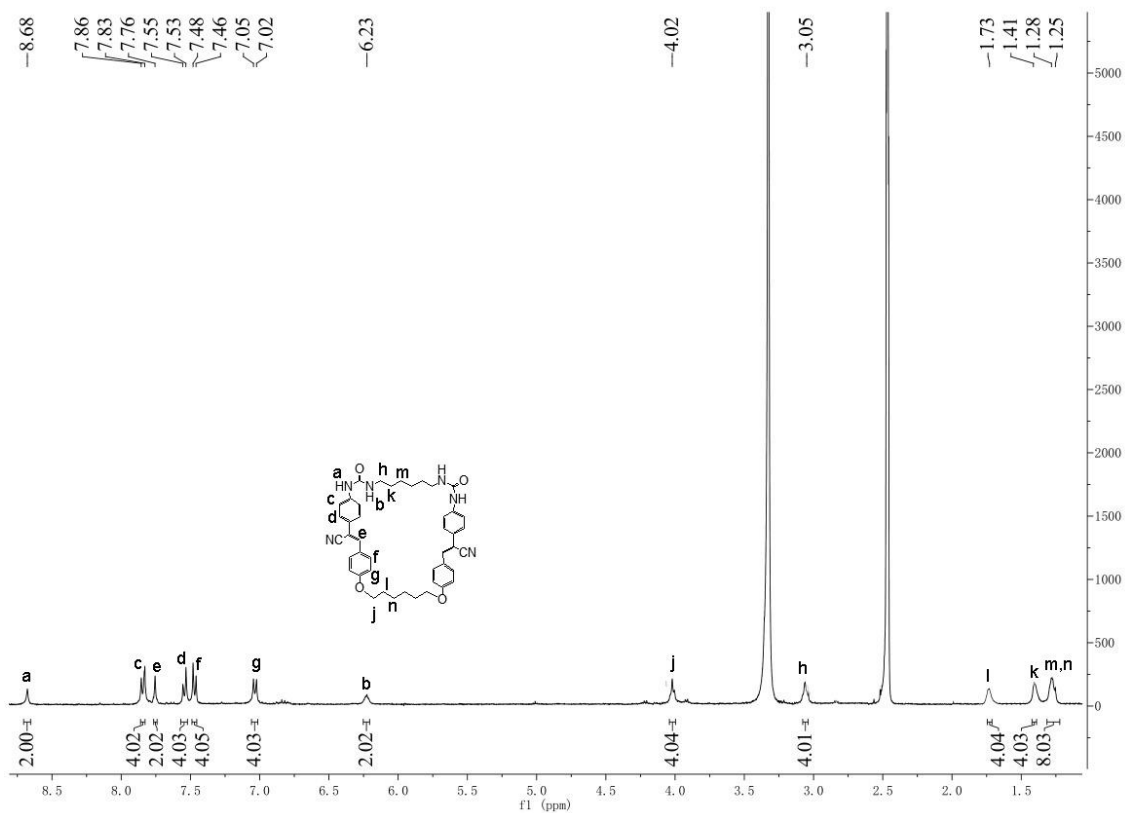Figure S2 MALDI-TOF-MS spectrum of compound **1**
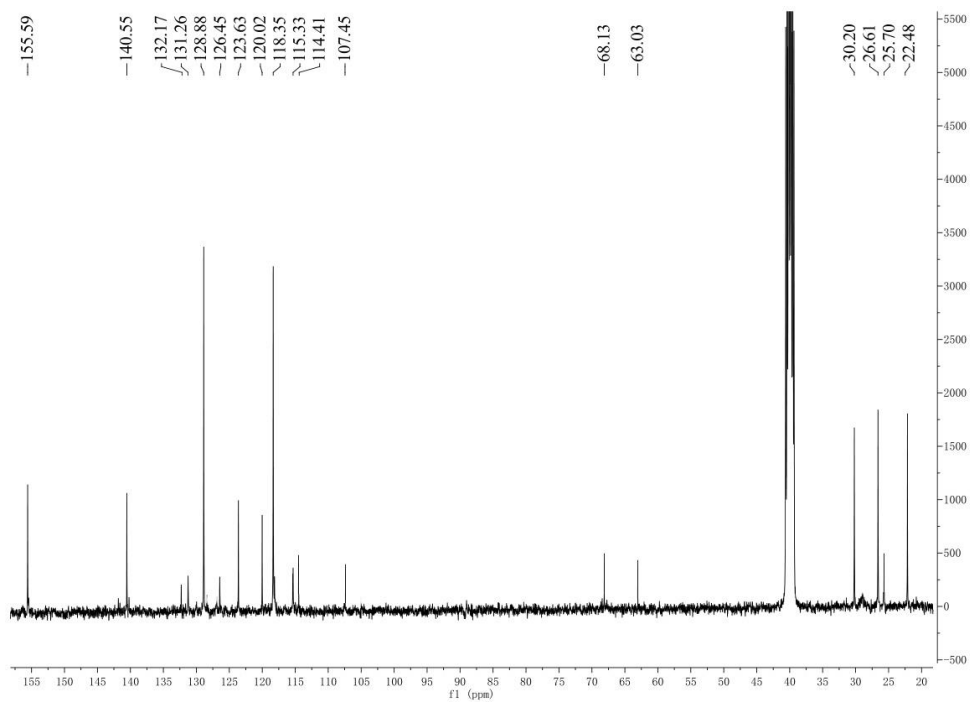

Figure S3 The ^{1}H NMR spectrum of compound **BCM**

Figure S4 The ^{13}C NMR spectrum of **BCM**

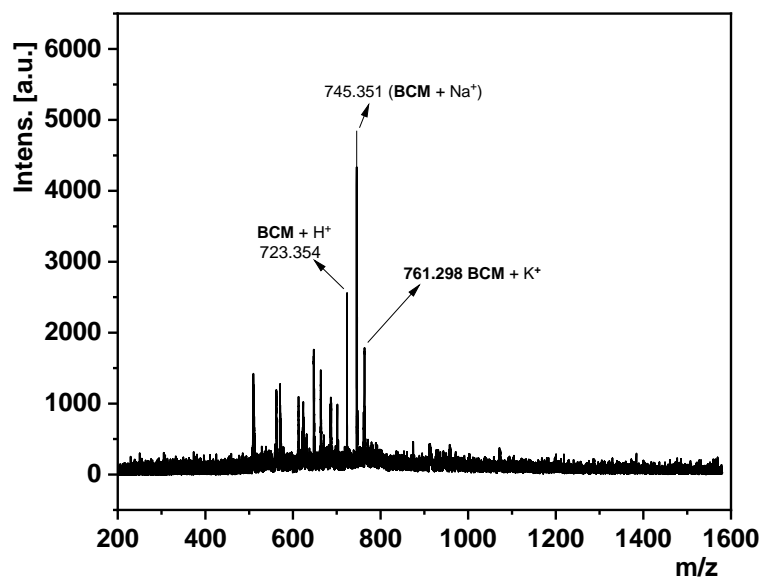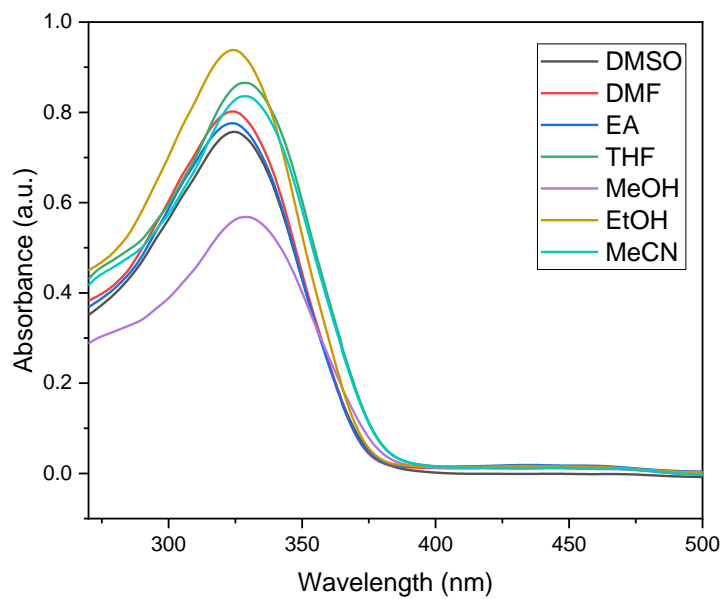

Figure S5 MALDI-TOF-MS spectrum of **BCM**

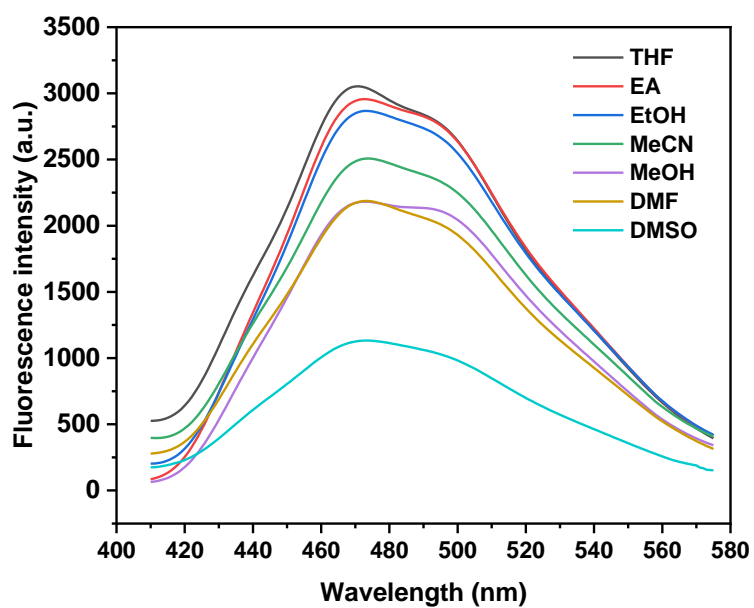Figure S6 The UV-Vis absorption spectra of **BCM** in different solvents (1.0×10^{-5} M)

Figure S7 Fluorescence spectra of **BCM** in different solvents (1.0×10^{-5} M, λ_{ex} = 340 nm)

Table S1: Comparison of DL values on detecting rutin hydrate

Detection method	Linear range	LOD	Reference
Electrochemical method	0.06-1.0 μM	0.68 nM	1
Electrochemical detection of graphite modification	1.0-150 nM	0.36 nM	2
HPLC-DAD-ESI-MS	/	0.1172 μg/mL	3
HPLC	0.05-50 mg L^{-1}	0.023 mg L^{-1}	4
Solid Phase Extraction - UV-Vis Spectrophotometry	1-90 μM	0.961 μM	5
HPLC	/	7.29 - 20.29 μg/mL	6
Photoelectrochemical detection of semiconductor nanomaterials	0.001nM-100 μ M	0.0007 nM	7
Quantum Dot Modified Electrodes - Photoelectrochemical Detection	0.025-50.0 μ M	0.007 μM	8
Colourimetric detection	770 n M- 54.46 μM	114 nM	9
Electrochemical polymerisation modified electrode detection	/	8.31 nM	10
Nitrogen and sulphur doped fluorescent probe detection	0-40 mg/L	0.02 μM	11
Fixed Dye Fluorescent Probes	2.0×10^{-6}-1.5×10^{-4} M	8.0×10^{-7} mol/L	12
Electrochemical method	0.02-50.00 μM	0.015 μmol/L	13
Electrochemical detection of nanomaterials	1.0225 μ A $\cdot$ μM$^{-1}\cdot$cm^{-2}	0.0027 μM	14
Water-soluble nanofluorescent probes	0.05 - 400 μM	15.2 nM	15
Quantum Dot Fluorescent Probes	5.0×10^{-7}-3.2×10^{-5} M	3.5×10^{-7} mol/L	16

HPLC-DAD	5-400 μg/mL	0.1-0.3 μg/mL	17
Fluorescence and electrochemical dual mode detection	$2.0\text{-}130.0 \times 10^{-8}$ M	0.076×10^{-8} M	18
MIP- Electrochemical method	1-400 nM	0.36 nM	19
Nanocomposite modified electrode	0.1-15 mM	0.26 nM	20
Fluorescence sesor in this work	0.1×10^{-5} M -1×10^{-4} M	1.16×10^{-7} M	This work

References

(1) Zhang, L.; Zhang, M.; Yang, P.; Zhang, Y.; Fei, J.; Xie, Y. Electrochemical Behavior of β-Cyclodextrin-Ni-MOF-74/Reduced Graphene Oxide Sensors for the Ultrasensitive Detection of Rutin. *Molecules* **2023**,28(12),4604.

(2) Xu, Y.; Chen, G.; Qin, Y.; Xiao, D. The Facile Activation of Graphite for the Improved Determination of Dopamine, Rutin and Acetamidophenol. *Analyst* **2023**,148,2100-2109.

(3) Junyou Shi; Jiang Hu; Zhiwei Sun. Comparative Study on Flavonoids from Tibetan Medicinal Plants Saussurea Species Using HPLC-DAD-ESI-MS. *J. Liq. Chromatogr. Relat. Technol.* **2023**,45,9-12.

(4) Jinyue Chai; Xue Chen; Chengcheng Jin; Fang Chai; Miaomiao Tian. Selective Enrichment of Rutin in Sunscreen by Boronate Affinity Molecularly Imprinted Polymer Prior to Determination by High Performance Liquid Chromatography. *Biochem. Eng. J.* **2023,**191,108811.

(5) Tabaraki, R.; Sadeghinejad, N. Preparation and Application of Magnetic Molecularly Imprinted Polymers for Rutin Determination in Green Tea. *Chem. Pap.* **2020**, *74* (6), 1937–1944.

(6) Jaiboonya Jaicharoensub; Intouch Sakpakdeejaroen; Sumalee Panthong. Validation of HPLC Method for Quantitative Determination of Active Compounds in Thai Traditional Herbal Medicine to Treat Gastrointestinal Disease. *Talanta Open* **2023**,7100227.

(7) Fatemeh Bakhnooh; Majid Arvand. A Novel "Signal-off" Photoelectrochemical Sensing Platform for Selective Detection of Rutin Based on Cu2SnS3/TiO2 Heterojunction. *J. Photochem. Photobiol. A Chem.* **2023**,439,114633.

(8) Wei, L.; Li, X.; Feng, S. A Photoelectrochemical Sensor for the Sensitive Detection of Rutin Based on a CdSe QDs Sensitized TiO2 Photoanode. *International Journal of Electrochemical Science* **2021**, *16* (1), 151032.

(9) Davoodi-Rad, K.; Shokrollahi, A.; Shahdost-Fard, F.; Azadkish, K. Copper-Guanosine Nanorods (Cu-Guo NRs) as a Laccase Mimicking Nanozyme for Colorimetric Detection of Rutin. *Biosensors* **2023**,13(3),374.

(10) B. Kanthappa; J. G. Manjunatha; N. Hareesha; Ammar M. Tighezza; Munirah D. Albaqami; Mika Sillanpää Electrochemically Polymerized DL-Phenylalanine-Deposited Graphene Paste Electrode for the Detection of Rutin. *ChemistrySelect* **2023**,8,7.

(11) Zhang, T.; Ji, Q.; Song, J.; Li, H.; Wang, X.; Shi, H.; Niu, M.; Chu, T.; Zhang, F.; Guo, Y. Preparation of Nitrogen and Sulfur Co-Doped Fluorescent Carbon Dots from Cellulose Nanocrystals as a Sensor for the Detection of Rutin. *Molecules* **2022** ,27(22),8021.

(12) Tan, S.-Z.; Hu, Y.-J.; Gong, F.-C.; Cao, Z.; Xia, J.-Y.; Zhang, L. A Novel Fluorescence Sensor Based on Covalent Immobilization of 3-Amino-9-Ethylcarbazole by Using Silver Nanoparticles as Bridges and Carriers. *Analytica Chimica Acta* **2009**, *636* (2), 205–209.

(13) Şenocak, A.; Sanko, V.; Tümay, S. O.; Orooji, Y.; Demirbas, E.; Yoon, Y.; Khataee, A. Ultrasensitive Electrochemical Sensor for Detection of Rutin Antioxidant by Layered Ti3Al0.5Cu0.5C2 MAX Phase. *Food Chem. Toxicol.* **2022**,164,113016.

(14) Raja Nehru; Chiu-Wen Chen; Mei-Ling Tsai; Cheng-Di Dong. Rational Design of Hexagonal Zinc Oxide/Boron-Doped g-C3N4 Nanosheets as Efficient Electrocatalyst for Enhanced Sensing of Rutin in Fruit Samples. *Colloids Surf. A Physicochem. Eng. Aspects* **2022**,655,130193.

(15) Pan, C.; Qin, X.; Lu, M.; Ma, Q. Water Soluble Silicon Nanoparticles as a Fluorescent Probe for Highly Sensitive Detection of Rutin. *ACS Omega* **2022**,32,28588-28596.

(16) Sun, Y.; He, W.; Sun, X.; Liu, B. MoS $_2$ Quantum Dots as a Specific Fluorescence Sensor for Selection of Rutin and for Temperature Sensing. *Luminescence* **2020**, *35* (8), 1416–1423.

(17) Basaraba, R.; Savych, A.; Marchyshyn, S.; Muzyka, N.; Ilashchuk, P. HPLC-DAD Assay of Phenols Profile in Antennaria Dioica (L.) Gaertn. *Pharmacia* **2022**,69(2),393-399.

(18) Ashraf M. Mahmoud; Mater H. Mahnashi; Adel Al Fatease; Mahmoud A.H. Mostafa; Mohamed M. El-Wekil; Ramadan Ali. Fluorometric and Electrochemical Dual-Mode Detection of Toxic Flavonoid Rutin Based on New Nitrogen and Sulfur Co-Doped Carbon Dots: Enhanced Selectivity Based on Masking the Interfering Flavonoids with BSA Complexation. *J. Food Compos. Anal.* **2022**,108,104428.

(19) Mahmoud, A. M.; El-Wekil, M. M.; Mahnashi, M. H.; Ali, M. F. B.; Alkahtani, S. A. Modification of N,S Co-Doped Graphene Quantum Dots with p-Aminothiophenol-Functionalized Gold Nanoparticles for Molecular Imprint-Based Voltammetric Determination of the Antiviral Drug Sofosbuvir. *Microchim Acta* **2019**, *186* (9), 617.

(20) Qin, D.; Li, T.; Li, X.; Feng, J.; Tang, T.; Cheng, H. A Facile Fabrication of a Hierarchical ZIF-8/MWCNT Nanocomposite for the Sensitive Determination of Rutin. *Anal. Methods* **2021**,13,5450-5457.
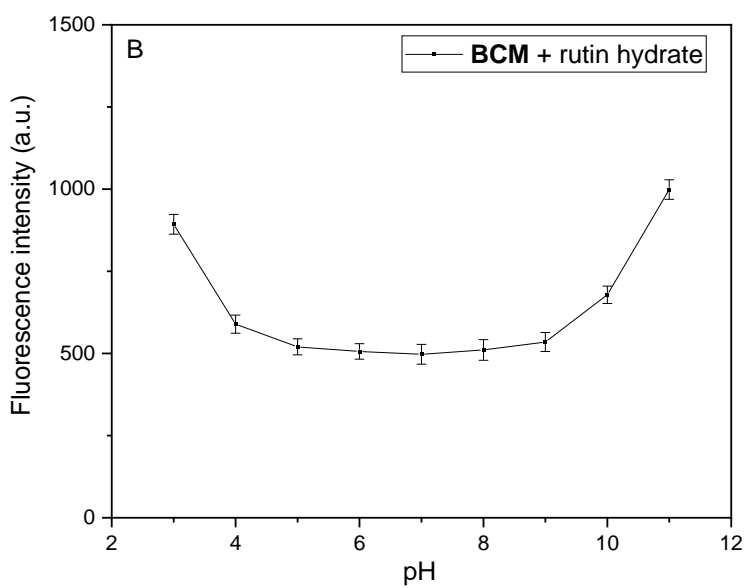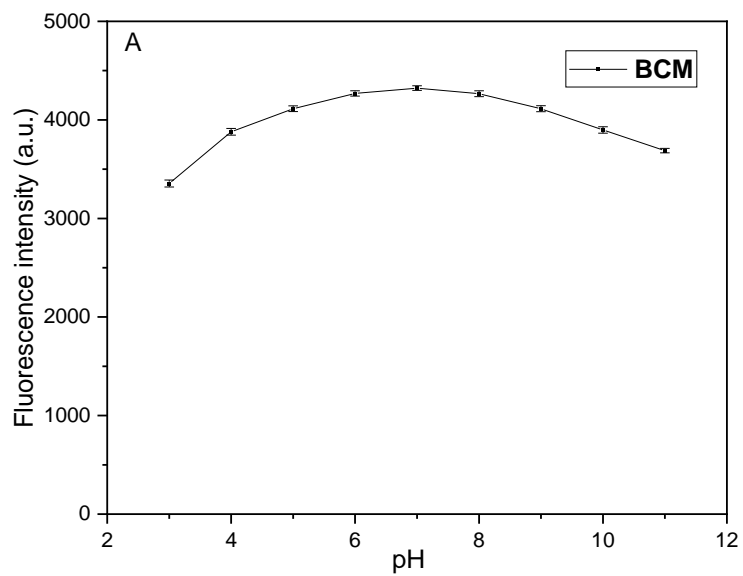
Figure S8 The influence of pH on the maximum fluorescence intensities of **BCM** (A) and **BCM** + rutin hydrate (B)**.** (λ_{ex} = 340 nm, 1.0×10^{-5} M each in DMSO-H$_2$O (5:95))
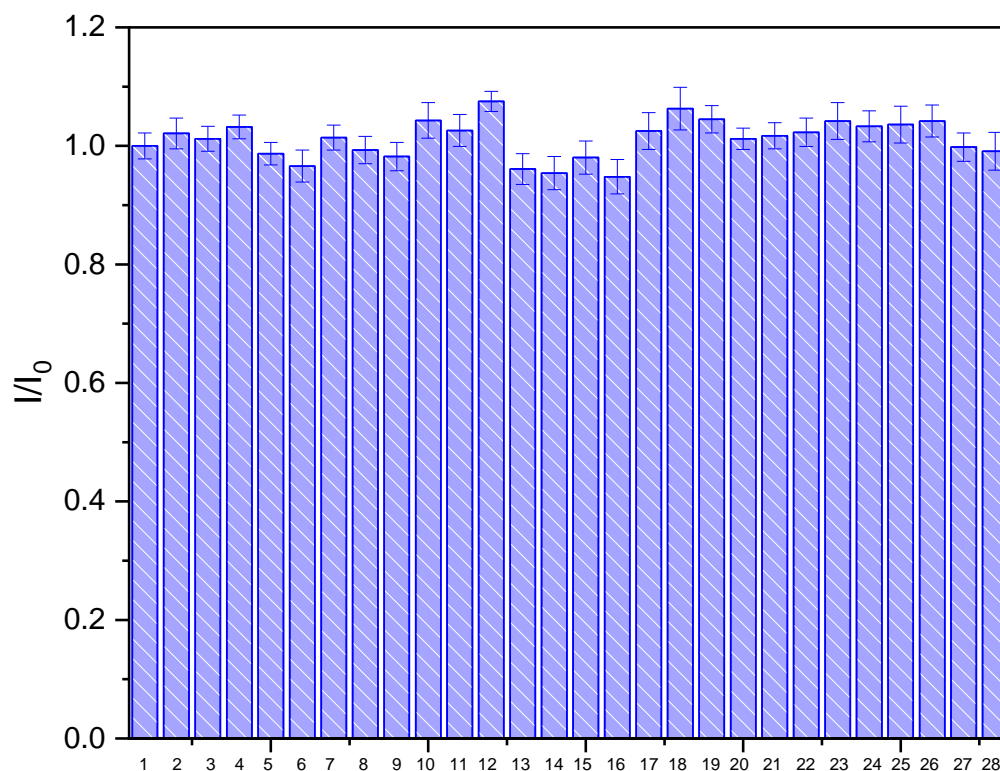
Figure S9 The interference experiments of **BCM** (1.0×10^{-5} M) with rutin hydrate in prescence of the interfering species (1×10^{-5} M each, λ_{ex} = 340 nm) in DMSO-H_2O (5:95). I_0 was the fluorescence intensity (λ_{em} = 475 nm) of **BCM** with rutin hydrate; I was the fluorescence intensity (λ_{em} = 475 nm) of **BCM** with rutin hyfrate in prescence of the interfering species. 1 = **BCM** + rutin hydrate, 2 = 1 + rutin hydrate, 3 = 1 + isonicotinic acid, 4 = 1 + niacin, 5 = 1 + thymine, 6 = 1 + adenine, 7 = 1 + VB12, 8 = 1 + VB1, 9 = 1 + rhamnose, 10= 1 + sorbic acid, 11 = 1 + D-fructose, 12 = 1 + lactose, 13 = 1 + Vitamin A acetate, 14 =1 + cytosine, 15 = 1 + glucose, 16 = 1 + citrate, 17 = 1 + ascorbic acid, 18 = 1 + methyl-man noside, 19 = 1 + amygdalin, 20 = 1 + folic acid, 21 = 1+ VC, 22 = 1 + Na^+, 23 = 1+ K^+, 24 = 1 + Fe^{3+}, 25 =1 + Mg^{2+}, 26 = 1 + Cu^{2+}, 27 = 1 + Ca^{2+}, 28 = 1 + Al^{3+}.
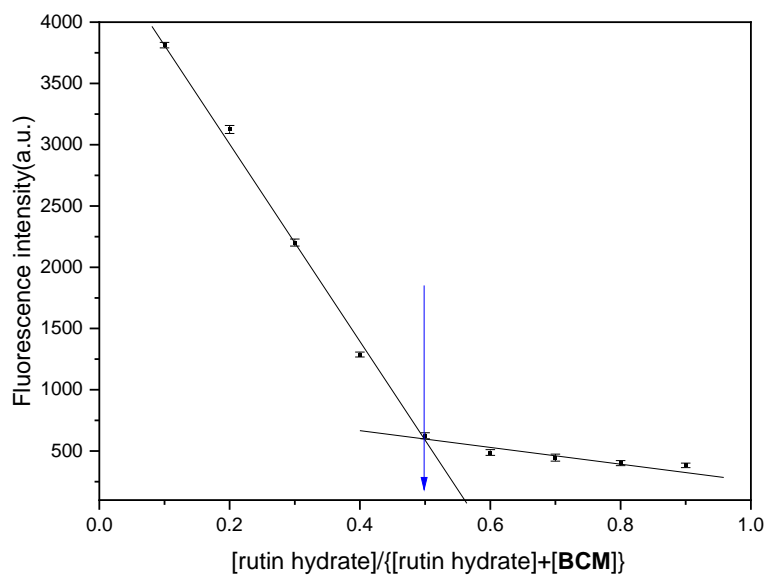
Figure S10 The Job's plot of **BCM** with rutin hydrate in DMSO-H$_2$O (5:95) (λ_{ex} = 340 nm) (The total concentration was 1.0×10^{-5} M)
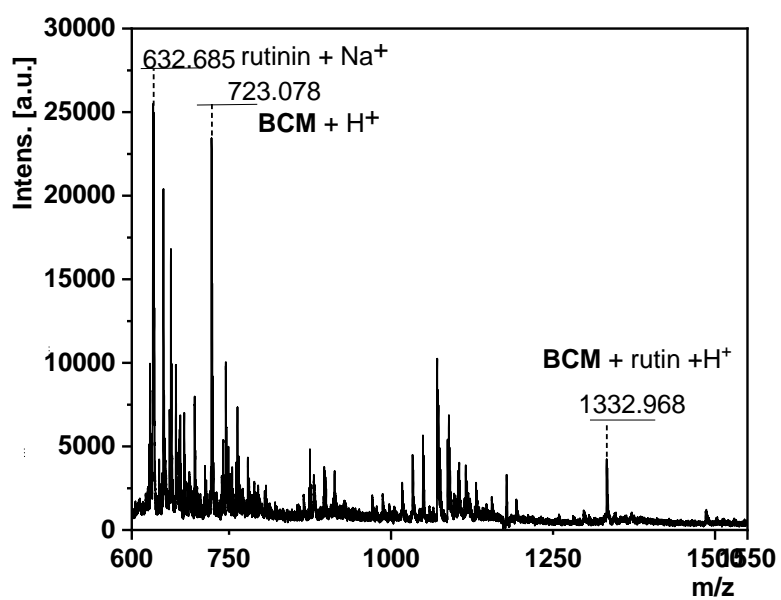
Figure S11 MALDI-TOF-MS spectrum of BCM with rutin hydrate (1:1).
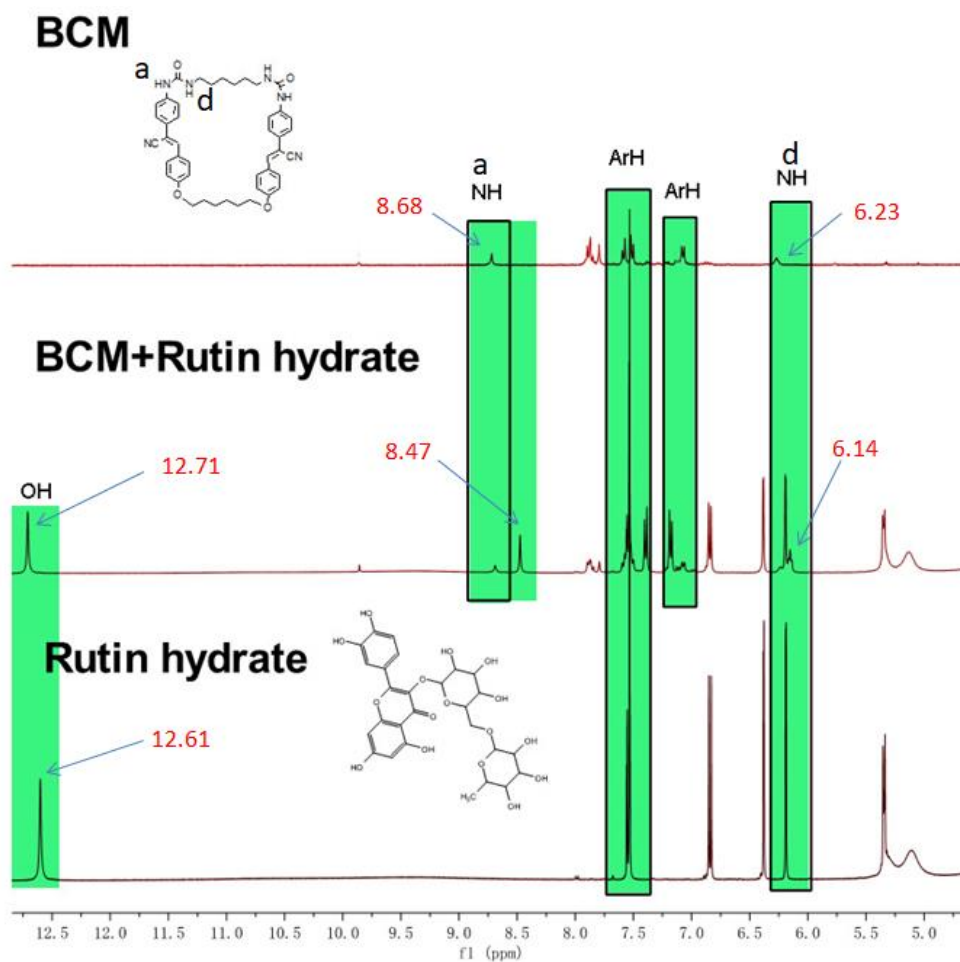
Figure S12 Comparison of ^{1}H NMR spectra of **BCM** with rutin hydrate (1:1).
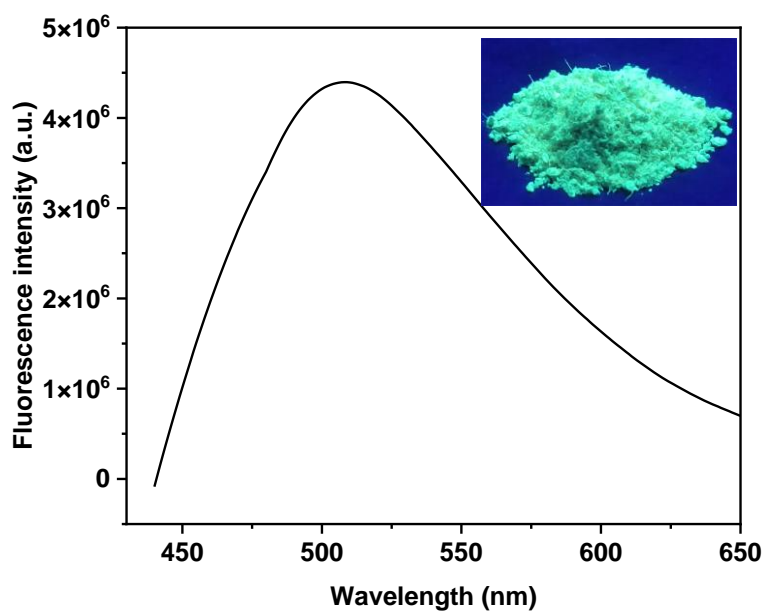
Figure S13 The fluorescence spectrum of **BCM** in solid film (λ_{ex} = 340 nm)
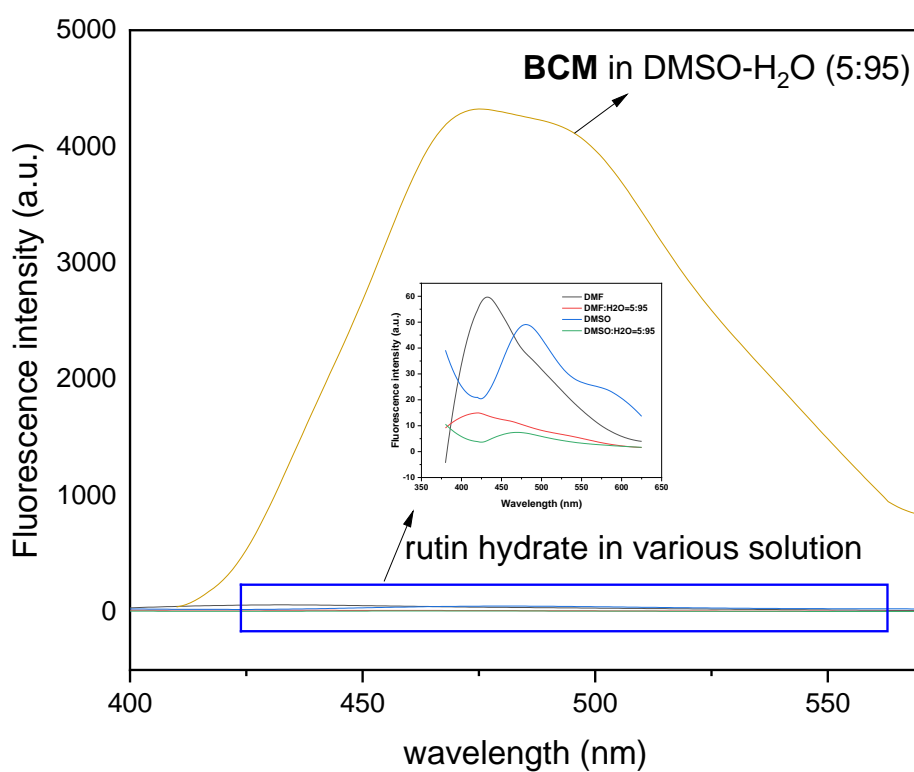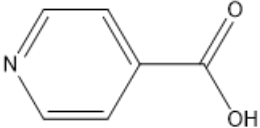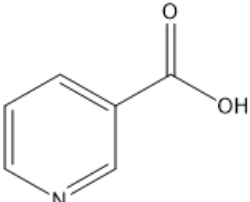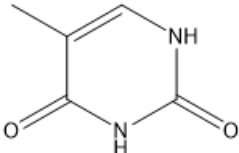
Figure S14 The comparison in fluorescence spectra of **BCM** and rutin hydrate

Table S2 Structural formula of the guest molecules

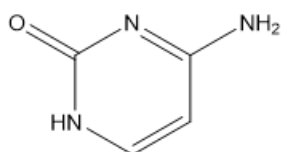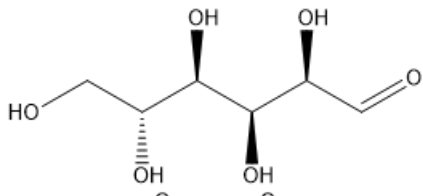| Structural formula of the guest molecule	Name of the object molecule	The guest molecule's corresponding ordinal number in Figure 2
	Isonicotinic acid	3
	Niacin	4
	Thymine	5
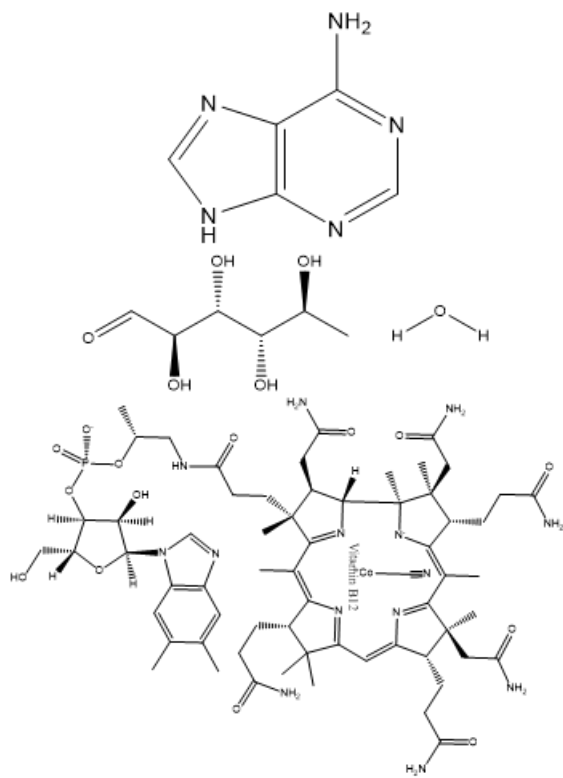
Adenine

6

Rhamnose

9

VB12

7
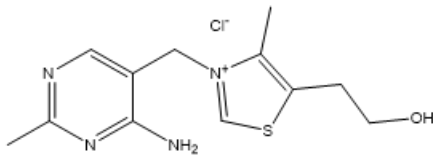
VB1

8
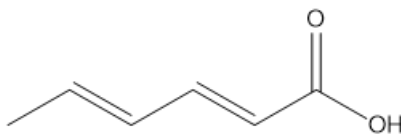
Sorbic acid

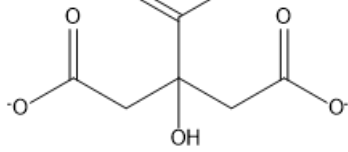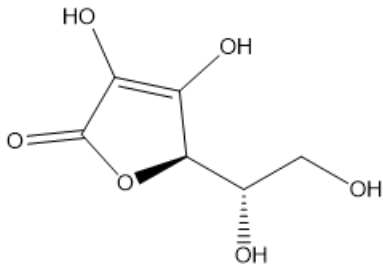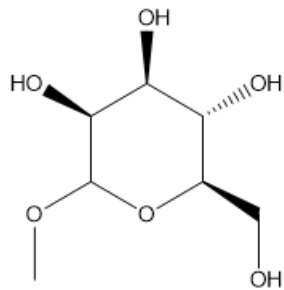10
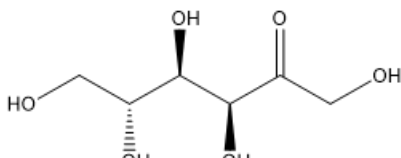
D-fructose

11
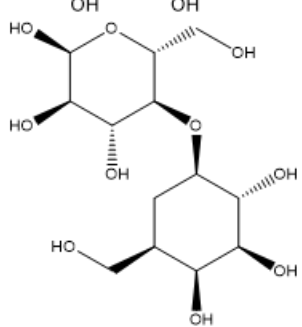
Lactose

12
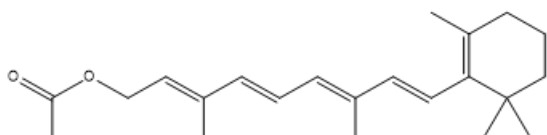
Vitamin A
acetate

13

Cytosine

14

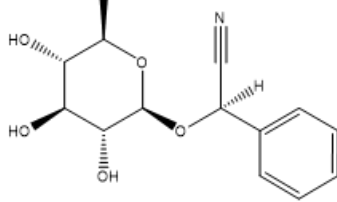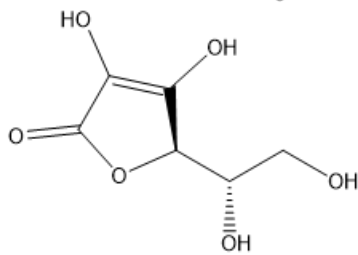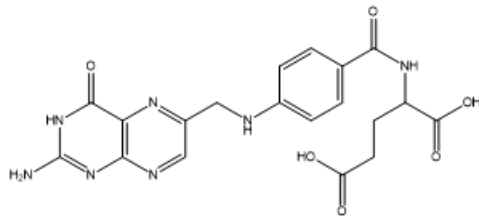|	
Glucose,	15
Citrate	16
Ascorbic acid	17
Methyl-man noside	18
Amygdalin	19
Folic acid	20
VC	21
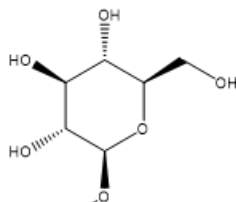
Calculation for Binding constant: The Benesi-Hildebrand formula: $(1/(I-I_0)=1/\{Ka(Imax-I_0)\times c[RT]\}-1/(Imax-I_0))$. The data were obtained as Figure S15, where the required binding constant is equal to the intercept divided by the slope: $2.4 \times 10^4\,M^{-1}$.

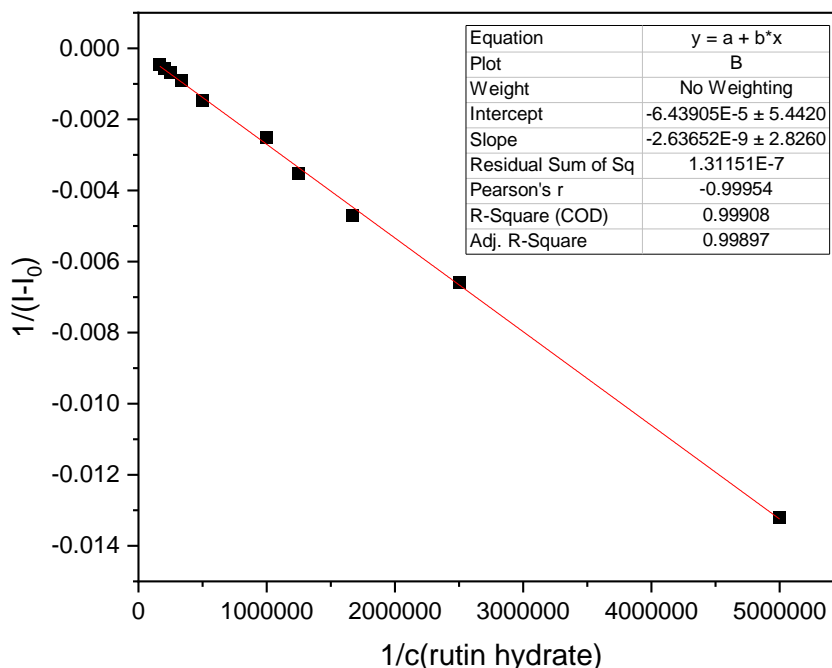| Equation	y = a + b*x
Plot	B
Weight	No Weighting
Intercept	-6.43905E-5 ± 5.4420
Slope	-2.63652E-9 ± 2.8260
Residual Sum of Sq	1.31151E-7
Pearson's r	-0.99954
R-Square (COD)	0.99908
Adj. R-Square	0.99897

Figure S15 Benesi-Hildebrand linear analysis curve of **BCM** for rutin hydrate

Calculation for detection limitation: According to the interpolation graph in Fig. 3 (B), a relatively good linear relationship between the fluorescence intensity of this probe and the change of concentration, was obtained with $R^2 = 0.99825$. Then we tested the fluorescence intensity of five sets of blank samples and obtained the relative standard deviation of the blank solution by calculation. Based on the formula of LOD=K×Sb1/S (K = 2 or 3, K was set 3 herein, Sb1 suggests the standard deviation of the blank solution and S means the slope of the standard curve), LOD was calculated as 1.16×10^{-7} M.

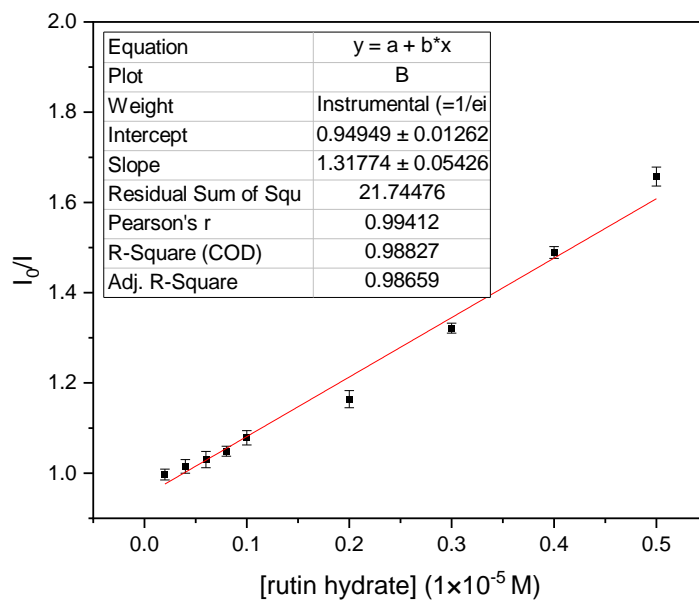| Equation	y = a + b*x
Plot	B
Weight	Instrumental (=1/ei
Intercept	0.94949 ± 0.01262
Slope	1.31774 ± 0.05426
Residual Sum of Squ	21.74476
Pearson's r	0.99412
R-Square (COD)	0.98827
Adj. R-Square	0.98659

Figure S16 Stern-Volner Quenching linear analysis curve of **BCM** for rutin hydrate

Calculation of quenching Constant: The Stern-Volmer Quenching Equation: $I_0/I=1+K_{sv}[M^{n+}]$ .The data obtained are shown in Fig. S16, and the quenching constant is equal to the slope: $1.32 \times 10^5 \, M^{-1}$.